

Search for neutrino emission in gamma-ray flaring blazars with the ANTARES telescope

Agustín Sánchez Losa on behalf of the ANTARES Collaboration

agustin.sanchez@ific.uv.es, IFIC, Apartado de Correos 22085, E-46071 Valencia, Spain

Abstract

The ANTARES telescope observes a full hemisphere of the sky all the time with a duty cycle close to 100%. This makes it well suited for an extensive observation of neutrinos produced in astrophysical transient sources. In the surrounding medium of blazars, i. e. active galactic nuclei with their jets pointing almost directly towards the observer, neutrinos may be produced together with gamma-rays by hadronic interactions, so a strong correlation between neutrinos and gamma-rays emissions is expected. The time variability information of the studied source can be obtained by the gamma-ray light curves measured by the LAT instrument on-board the Fermi satellite. If the expected neutrino flux observation is reduced to a narrow window around the assumed neutrino production period, the point-source sensitivity can be drastically improved. The ANTARES data collected in 2008 has been analysed looking for neutrinos detected in the high state period of ten bright and variable Fermi sources assuming that the neutrino emission follows the gamma-ray light curves. First results show a sensitivity improvement by a factor 2-3 with respect to a standard time-integrated point source search. The analysis has been done with an unbinned method based on the minimization of a likelihood ratio applied to data corresponding to a live time of 60 days. The width of the flaring periods ranges from 1 to 20 days. Despite the fact that the most significant studied source is compatible with background fluctuations, recently detected flares promise interesting future analyse.

Keywords: ANTARES, Neutrino astronomy, Fermi transient sources, time-dependant search, blazars

1. Introduction

Neutrino astronomy is an incipient field of observation of the universe. Since neutrinos do not interact electromagnetically, but weakly only, they are not absorbed and point directly to their original sources, playing the role of unique messengers. However, due to their weak interaction, neutrino telescopes are very low event rate experiments requiring high fluxes in order to detect a clear signal of a neutrino astrophysical source. Up to now no claim of an astronomy source of neutrinos further than the Sun has been made, with the exception of the well known SN1987A. Assuming a direct correlation between the neutrino emission and the light emission of a source in an hadronic acceleration scenario [1], the standard analysis can be improved by a factor 2–3 in the sensitivity if we limit this search to the periods of maximum probability of neutrino emission by the source. The time variability visible in the gamma-ray light curves measured by the Fermi-LAT [2] can be used for this purpose.

1.1. The ANTARES telescope

The ANTARES detector is a neutrino telescope placed at the bottom of the Mediterranean Sea ($42^{\circ}48\text{ N}$, $6^{\circ}10\text{ E}$), at a depth of 2475 m, connected by a submarine cable of 42 km to the shore in Toulon (France). This cable connects

through a junction box 12 lines which are separated by 60–70 m and vertically suspended by a buoy. Each line has 25 floors spaced by 14.5 m, except for line 12 which has only 20 floors. A floor consists of a triplet of optical modules (OMs) each one housing a photomultiplier (PMT) facing 45° downwards. The full detector is a tri-dimensional array of 885 PMTs [3] [4] which was completed in 2008 when the last line was connected.

Neutrinos are detected via the Cherenkov light induced by relativistic muons produced in the detector surroundings by CC interactions of muon neutrinos with nuclei in water. The signals from the Cherenkov photons detected by the PMTs are digitized (‘hits’) [5] and sent to the shore station for reconstruction and physics analysis.

2. Time-dependent analysis

2.1. Analyzed data

The analyzed data correspond to the period from September 6th to December 31st, 2008 (54720–54831 modified Julian day). Some periods have been excluded from the selection in order to avoid conditions with high optical backgrounds due to the bioluminescence activity, leaving 60.8 days of life-time.

While most of the atmospheric muon background is suppressed by selecting only up-going events, a fraction

of mis-reconstructed events still remains which have to be rejected in a different way. In the track-reconstruction process an algorithm based on the maximization of a likelihood is used. The likelihood function is built from the difference between the expected and the measured arrival times of the hits from the Cherenkov photons emitted along the muon track. Its maximization considers the Cherenkov photons that scatter in the water and the additional photons that are generated by secondary particles (e.g. electromagnetic showers created along the muon trajectory). A good measure of the track-fit quality is the value of the log-likelihood per degree of freedom (λ), providing a useful tool to reject the mis-reconstructed muons by applying a cut in that λ value. This cut leaves the atmospheric neutrinos as the dominant background. An additional cut requiring the error estimated for the reconstructed muon track direction to be less than 1° is also applied in the selection of events.

The angular resolution has been estimated by Monte Carlo simulations. The cumulative distribution of the angular difference between the reconstructed muon direction and the neutrino direction, with an assumed spectrum proportional to E_ν^{-2} , where E_ν is the neutrino energy, is shown in Fig. 1. For the studied period, the median resolution is estimated to be 0.4 ± 0.1 degrees.

2.2. Time-dependent search algorithm

An unbinned method based on a likelihood ratio maximization has been used to perform this time-dependent point-source analysis. The data is parameterized as a two components mixture of signal and background. The goal is to determine, at a given point in the sky and at a given time, the relative contribution of each component and to calculate the probability to have a signal above a given background model. The likelihood ratio λ is the ratio of the probability density for the hypothesis of background and signal ($H_{\text{sig}+\text{bkg}}$) over the probability density of only background (H_{bkg}):

$$\lambda = \sum_{i=1}^N \log \frac{P(x_i | H_{\text{sig}+\text{bkg}})}{P(x_i | H_{\text{bkg}})} \quad (1)$$

$$= \sum_{i=1}^N \log \frac{\frac{n_{\text{sig}}}{N} P_{\text{sig}}(\alpha_i, \delta_i, t_i) + (1 - \frac{n_{\text{sig}}}{N}) P_{\text{bkg}}(\alpha_i, \delta_i, t_i)}{P_{\text{bkg}}(\alpha_i, \delta_i, t_i)}$$

where n_{sig} and N are respectively the unknown number of signal events and the total number of events in the considered data sample. $P_{\text{sig}}(\alpha_i, \delta_i, t_i)$ and $P_{\text{bkg}}(\alpha_i, \delta_i, t_i)$ are the probability density function (PDF) for signal and background respectively, and δ_i is the declination of the studied source. For a given event i , t_i and α_i represent the time of the event and the angular difference between the coordinate of this event and the studied source.

$P_{\text{sig}}(\alpha_i, \delta_i, t_i)$ and $P_{\text{bkg}}(\alpha_i, \delta_i, t_i)$ are described by two components:

$$P_{\text{sig}}(\alpha_i, \delta_i, t_i) = P_{\text{sig}}^{\text{dir}}(\alpha_i, \delta_i) \times P_{\text{sig}}^{\text{time}}(t_i) \quad (2)$$

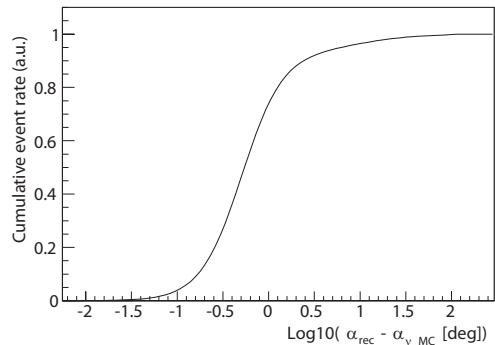


Figure 1: Cumulative distribution of the angle between the true Monte Carlo neutrino direction and the reconstructed muon direction for E^{-2} upgoing neutrino events selected for this analysis.

$$P_{\text{bkg}}(\alpha_i, \delta_i, t_i) = P_{\text{bkg}}^{\text{dir}}(\alpha_i, \delta_i) \times P_{\text{bkg}}^{\text{time}}(t_i)$$

where $P_{\text{sig}}^{\text{dir}}$ is the probability to have a signal event from the studied source, computed via Monte Carlo, $P_{\text{sig}}^{\text{time}}$ is the probability of a neutrino event derived from the gamma-ray light curve correlation, and $P_{\text{bkg}}^{\text{dir}}$ and $P_{\text{bkg}}^{\text{time}}$ are the corresponding background PDFs. The shape of the time PDF for the signal event, $P_{\text{sig}}^{\text{time}}$, is extracted directly from the gamma-ray light curve assuming that it is proportional to the gamma-ray flux. For the signal event directional PDF, $P_{\text{sig}}^{\text{dir}}$, the one-dimensional point-spread function is used, which is the probability density of reconstructing an event at an angular distance α_i from the true source position. Then, the directional, $P_{\text{bkg}}^{\text{dir}}$, and time PDF for the background, $P_{\text{bkg}}^{\text{time}}$, are derived from the data using respectively the observed declination distribution of selected events in the sample and the observed time distribution of all the reconstructed muons. The latter distribution (not normalized to 1) is shown in Fig. 2, where periods without data (due to detector maintenance, etc) or with very poor quality data (high bioluminescence activity or bad calibration) are shown as empty bins.

The λ_{data} value obtained from the data is then compared to the distribution of λ given by the null hypothesis ($n_{\text{sig}} = 0$). The comparison of λ_{data} with the background only λ distribution is used to reject the null hypothesis, where the confidence level corresponds to the fraction of the scrambled trials above λ_{data} (p-value). The discovery potential is then defined as the average number of signal events required to achieve a p-value lower than the equivalent to 5σ in 50% of trials.

The average number of events required for a 5σ discovery (50% C.L.) produced in one source located at a declination of -40° as a function of the total width of the flare period is shown in Fig. 3. A comparison with the numbers obtained with a standard time-integrated point source search, shows an improvement of the discovery potential by about a factor 2–3.

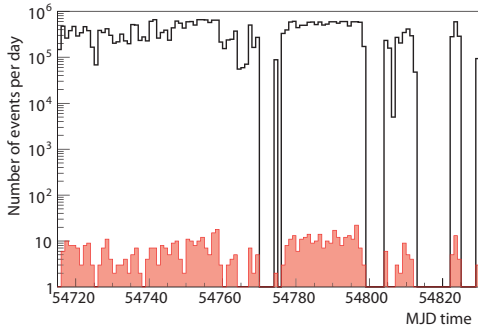


Figure 2: Time distribution of the reconstructed events. Black: distribution for all reconstructed events. Red filled: distribution of selected upcoming events ($\lambda > -5.4$ and $\beta < 1^\circ$). If 0, there are no data available (i. e. detector in maintenance) or the data have a very poor quality (high bioluminescence or bad calibration).

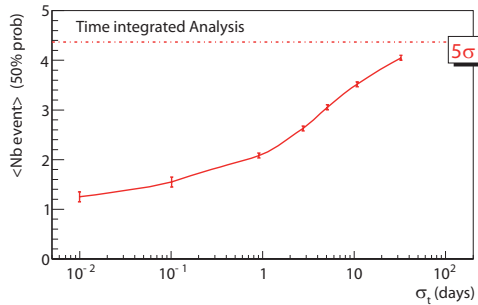


Figure 3: Average number of events required for a 5σ discovery (50% C.L.) of a source located at a declination of -40° as a function of the width of the flare period (solid line), a simple Heavyside function. This is compared to the number required for a time-integrated search (dashed line). The average typical length of the studied source flares goes from 1 up to 100 days.

2.3. Search for neutrino emission from gamma-ray flares

The sources for which this time-dependent analysis has been applied have been selected from the Fermi blazar sources reported in the first year Fermi LAT catalogue [6] and in the LBAS catalogue (LAT Bright AGN sample [7]). The selection has been done based on their variability, brightness and visibility: sources visible to ANTARES with a significant time-variability in the studied period and a flux in the high state greater than 20×10^{-8} photons $\text{cm}^{-2}\text{s}^{-1}$ above 300 MeV in the averaged 1 day-binned light curve were selected. The final selection list of sources includes four BLLacs and six flat spectrum radio quasars (FSRQ), listed in Table 1. Table 1 lists their fluxes, visibility and live times.

The light curves used for $P_{\text{sig}}^{\text{time}}$ in (2) are those published on the Fermi web page for monitored sources [8] (one-day-binned time evolution of the average gamma-ray flux above a threshold of 100 MeV). Figure 4 shows the high state periods (blue histogram) obtained for the Fermi

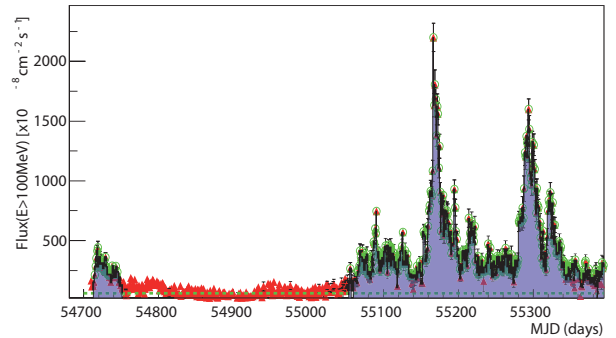


Figure 4: Gamma-ray light curve (red dots) of the blazar 3C454.3 measured by the LAT instrument on board the Fermi satellite above 100 MeV for almost two years of data. Blue histogram: high state periods. Green line and dots: baseline and significant points above this baseline used for the determination of the flare periods.

LAT gamma-ray light curve of 3C454 for almost two years of data. These states are defined using a simple and robust method based on three steps:

- First, the baseline and its error is determined with an iterative linear and gaussian fits. After each fit, the points where the flux is above the fitted base line plus one sigma are suppressed. This is done 3 times.
- Then all points (green dots in Fig. 4) where the measured flux minus its error is above the baseline plus two times the baseline sigma and at the same time the measured flux value is above the baseline plus three times the baseline sigma, are used as priors from which the flares are defined.
- Then, for each selected prior, the adjacent points for which the emission is compatible with a flare are added, i. e. the adjacent points which have their flux minus their error above the baseline plus one sigma. Finally, an additional delay of 0.5 days is added before and after the flare in order to take into account the 1-day binning of the light curve. Hence, a flare has a minimum width of 2 days.

Assuming that the neutrino emission follows that in gamma-rays, the signal time PDF is simply this de-noised light curve after normalization.

3. Results

The most significant source is 3C279, which has a pre-trial p-value of 1.03%. The unbinned method finds one high-energy neutrino event located 0.56° from the source location during a large flare in November 2008 (Fig. 4). This event has been reconstructed with 89 hits spread on 10 lines with a track fit quality $\lambda = -4.4$ and an error estimate of $\beta = 0.3^\circ$. The post-trial probability is computed

Source	OFGL name	Class	Redshift	F_{300}	Visibility	Live Time	$N(5\sigma)$	N_{obs}	Fluence
PKS 0208-512	J0210.8-5100	FSRQ	1.003	4.43	1.00	8.8	4.5	0	2.8
AO 0235+164	J0238.6+1636	BLLac	0.940	13.19	0.51	24.5	4.3	0	18.7
PKS 0454-234	J457.1-2325	FSRQ	1.003	13.56	0.63	6.0	3.3	0	2.9
OJ 287	J0855.4+2009	BLLac	0.306	2.48	0.39	4.3	3.9	0	3.4
WComae	J1221.7+28.14	BLLac	0.102	2.58	0.33	3.9	3.8	0	3.6
3C 273	J1229.1+0202	FSRQ	0.158	8.68	0.49	2.4	2.5	0	1.1
3C 279	J1256.1-0548	FSRQ	0.536	15.69	0.53	13.8	5.0	1	2.8
PKS 1510-089	J1512.7-0905	FSRQ	0.360	28.67	0.55	4.9	3.8	0	2.8
3C 454.3	J2254.0+1609	FSRQ	0.859	24.58	0.41	30.8	4.4	0	23.5
PKS 2155-304	J2158.8-3014	BLLac	0.116	7.89	0.68	3.1	3.7	0	1.6

Table 1: List of the bright, variable Fermi blazars selected for this analysis. F_{300} is the gamma-ray flux above 300 MeV in 10^{-8} photons cm^2s^{-1} . Live Time is the effective time of observation of the source in days. $N(5\sigma)$ are the number of neutrino events needed to be detected in ANTARES with 5σ , while N is the number of events observed in the source's direction and flare time window. Fluence is the upper limit (90% C.L.) on the neutrino fluence in GeV cm^{-2} , calculated according to the classical (frequentist) method for upper limits [9].

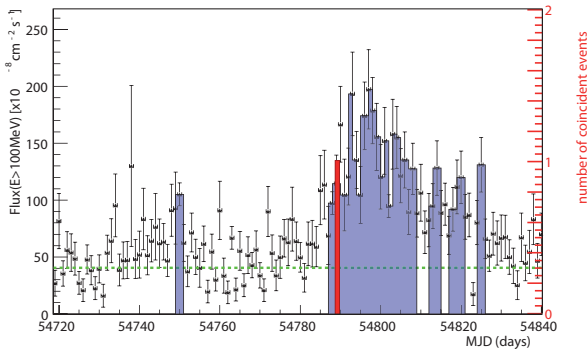


Figure 5: Gamma-ray light curve (black dots) of the blazar 3C279 measured by the LAT instrument on board the Fermi satellite above 100 MeV. Blue histogram: high state periods. Green dashed line: fit of a baseline. Red histogram: time of the ANTARES neutrino event in coincidence with 3C279.

taking into account the ten searches. The final probability of 10% is compatible with a background fluctuation. Other source results are summarized in Table 1.

4. Conclusion

The first time-dependent search for cosmic neutrinos in ANTARES has been presented. It has used data taken with the full 12-line ANTARES detector during the last four months of 2008. Time-dependent searches are significantly more sensitive than a standard point-source search for a variable source. This search has been applied to ten bright and variable Fermi LAT blazars. The most significant observation of a flare is 3C279 with a p-value of about 10% after trials for which one neutrino event has been detected in time and space coincident with the gamma-ray emission. Limits on the neutrino fluence have been obtained for the ten selected sources. The most recent measurements of Fermi in 2009-11 show very large flares

yielding a more promising search for neutrinos [10], and ongoing analyses are being performed together with improvements in the denoising of the light curves.

5. Acknowledgments

We gratefully acknowledge the financial support of the Spanish Ministerio de Ciencia e Innovación (MICINN), grants FPA2009-13983-C02-01, ACI2009-1020 and Consolider MultiDarkCSD2009-00064 and of the Generalitat Valenciana, Prometeo/2009/026.

References

- [1] T.K. Gaisser, F. Halzen, T. Stanev, Phys. Rep. 258 (1995) 173; J.G. Learned, K. Mannheim, Ann. Rev. Nucl. Part. Sci. 50 (2000) 679; F. Halzen, D. Hooper, Rep. Prog. Phys. 65 (2002) 1025.
- [2] A.A. Abdo et al., Astrophys. J. 722 (2010) 520.
- [3] J.A. Aguilar et al., ANTARES Collaboration, Nucl. Instrum. Meth. A 570 (2007) 107.
- [4] J.A. Aguilar et al., ANTARES Collaboration, Astropart. Phys. 34 (2011) 539.
- [5] J.A. Aguilar et al., Nucl. Instr. Meth. A622 (2010) 59.
- [6] A.A. Abdo et al., Astrophys. J. Suppl. 188 (2010) 405.
- [7] A.A. Abdo et al., Astrophys. J. 715 (2010) 429.
- [8] <http://fermi.gsfc.nasa.gov/ssc/data/access/lat/> (last access: 28th of February, 2012)
- [9] J. Neyman, Phil. Trans. Royal Soc. London Series A 236 (1937) 333.
- [10] A.A. Abdo et al., Astrophys. J. Lett. 733 (2011) L26; M. Ackermann et al., Astrophys. J. 721 (2010) 721; A.A. Abdo et al., Astrophys. J. 721 (2010) 1425; A.A. Abdo et al., Astrophys. J. Lett. 714 (2010) L73.